Semiconductor Physics, Quantum Electronics & Optoelectronics, 2012. V. 15, N 1. P. 65-71.

PACS 72.40.+w, 77.65.Ly, 81.05.Dz

Narrow-gap piezoelectric heterostructure as IR detector

F.F. Sizov[1], A.B. Smirnov[1], R.K. Savkina[1], V.A. Deriglazov[1], and M.V. Yakushev[2]
[1]*V. Lashkaryov Institute of Semiconductor Physics, NAS of Ukraine,*
41, prospect Nauky, 03028 Kyiv, Ukraine
Phone: (044) 525-1813; fax: (044) 525-1810
E-mail: alex_tenet@isp.kiev.ua; r_savkina@isp.kiev.ua
[2]*Institute of Semiconductor Physics, SB RAS,*
13, Lavrentyeva Av., 630090 Novosibirsk, Russian Federation

Abstract. Narrow-gap mercury cadmium telluride thin films grown by MBE and LPE methods onto various substrates (HgCdTe/Si, HgCdTe/GaAs, HgCdTe/CdZnTe) were investigated as a piezoelectric heterostructure for IR detection. The photoresponse, infrared transmittance spectra, parameters of the charge carrier transport, and mechanical properties were studied. Mechanical stresses at the layer-substrate interface were analyzed. HgCdTe-based infrared device is considered, operating in the middle (3–5 μm) infrared spectral range without cryogenic cooling to achieve performance level $D^* = 2.6 \cdot 10^9\ \mathrm{W}^{-1}\mathrm{cm} \cdot \mathrm{Hz}^{1/2}$. The possibility to detect infrared radiation is thought to be based on the possibility of the spatial separation of the non-equilibrium carriers in the strained semiconductor heterostructure with piezoelectric properties.

Keywords: IR detector, strained heterostructure, piezoelectric properties, HgCdTe.

Manuscript received 29.12.11.; revised version received 11.01.12; accepted for publication 26.01.12; published online 29.02.12.

1. Introduction

HgCdTe (MCT) is a variable-gap semiconductor, which is used most often in the production of infrared (IR) photon detectors [1]. It follows from both fundamental considerations and material flexibility. The basic research is focused on the growth, doping and characterization of MCT on CdZnTe substrate with 4% zinc concentration for lattice matching, because the highest crystal perfection is realized only for this material compound [1]. The most attractive among alternative substrates, which have the advantages in comparison with CdZnTe substrates from the viewpoint of substrate dimensions and low cost, are those based on GaAs [2] and Si [2-5]. The disadvantage of these substrates is a large lattice mismatch of compound materials, which is equal to ~14.6% for CdTe/GaAs and ~19% for CdTe/Si at room temperatures (see Table 1). It leads to a decrease in MCT crystalline perfection and to occurrence of the significant misfit deformation in comparison with the use of CdZnTe substrates.

Another problem associated with MCT detectors is the operating temperature. Traditionally, IR imaging is based on photodetectors fabricated from compound semiconducting films, which require a specific cooling system to minimize the effects of internal thermal noise and to operate at a temperature where they exhibit the maximum detection, fast refresh rates, small focusing optics and can have a high resolution because of small pixel size in arrays. Cooling requirements increase the price and size of IR systems. Moreover, when MCT devices are cooled from room to cryogenic temperatures, thermal stresses are introduced due to mismatch in the coefficients of thermal expansion of MCT and substrate (see Table 1).

Thus, stresses and strains accompany this material from the growth phase to fabrication and operation of devices.

© 2012, V. Lashkaryov Institute of Semiconductor Physics, National Academy of Sciences of Ukraine

Under normal conditions, MCT crystallizes in $F43m$ lattice and has one independent piezoelectric constant e_{14}. Therefore, mechanical stresses can induce electric fields and/or surface charges in MCT due to piezoelectric effects [8]. This field may have adverse effects on HgCdTe devices – efficiently magnify or suppress *p-n* junction-based fields specifically [8, 9]. At the same time, the piezoelectric effect in II-VI strained heterostructures can lead to large changes in optical properties and can have interesting applications in electro-optics or nonlinear optics [10, 11]. These electric fields can also cause charge accumulation, which can be used in the field effect transistor [12] and resonant tunneling structures. Strain-induced piezoelectric effects in arbitrary shaped II-VI quantum wire are presented in [13].

In this work, we describe the possibility to detect IR radiation by a piezoelectric heterostructure of HgCdTe on Si, operating in the middle (3–5 µm, MWIR) and longwave (8–14 µm, LWIR) spectral ranges without cryogenic cooling to achieve useful performance [14].

2. Experiment

2.1. MCT-based heterostructures growth

MCT-based heterostructures were grown by MBE with intermediate CdTe/ZnTe buffer layers on [310]-oriented Si substrates and [013]-oriented GaAs substrates [2]. A schematic of the MCT-based heterostructure is shown in Fig. 1a. The growth temperature was within T = 200…240 °C for ZnTe nucleation layers and T = 280…320 °C for CdTe buffer layers.

To decrease the influence of surface recombination, MCT layers were grown with x increasing in direction to the surface [2]. Close to the buffer layer, the Cd content also increases, and a potential barrier can be formed in some cases between the buffer and photosensitive layers. During the growth process, the composition of the layer was controlled by a built-in ellipsometer. Typical MCT composition profile throughout the thickness is shown in Fig. 1b.

Semi-insulating $Cd_{1-x}Zn_xTe$ wafers were used as substrates for LPE-grown *p*-type MCT layers. $Hg_{0.74}Cd_{0.26}Te$ epilayers were grown on [111]-oriented $Cd_{0.96}Zn_{0.04}Te$ substrates from a Te-rich solution at 450 °C.

2.2. Characterization of MCT-based heterostructures

We have carried out a systematic study of mercury cadmium telluride layers. Parameters of the charge carrier transport, infrared transmittance spectra, and mechanical properties of MCT-based heterostructures grown onto various substrates were studied.

MBE as-grown undoped MCT films have *n*-type conductivity regardless of the substrate (GaAs or Si). Structures of *p*-type conductivity were obtained by isothermal annealing in helium atmosphere at the annealing temperature 230 °C, mercury temperature 30 °C and the duration of annealing 20 hours.

The concentration and mobility of carriers in MCT layers were determined from measurements of the Hall coefficient R_H and conductivity σ, which were made by the van-der-Pauw method in magnetic field with B varying from 0.01 to 0.7 T at 78 K. These data are summarized in Table 2. The high resistivity of substrates excluded any influence on the results of electrical measurements. According to calculations in Ref. 15, the effect of the wide-band layer on the experimental electrophysical parameters can be neglected.

The infrared transmittance spectra of MCT-based heterostructures were obtained under illumination from the MCT layer side by traditional FTIR transmission analysis (Fig. 2). They are close to the theoretical one, and their absorption edge can be used to determine the MCT composition. Oscillations in the transmittance of MCT/Si and MCT/GaAs structures are induced by the interference of radiation inside the multilayer structure.

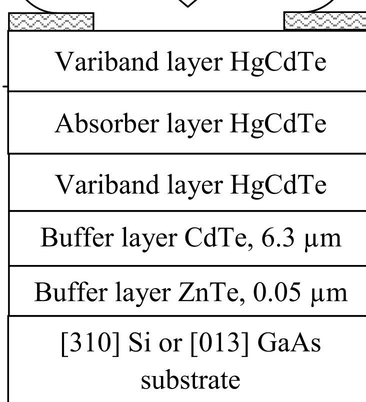

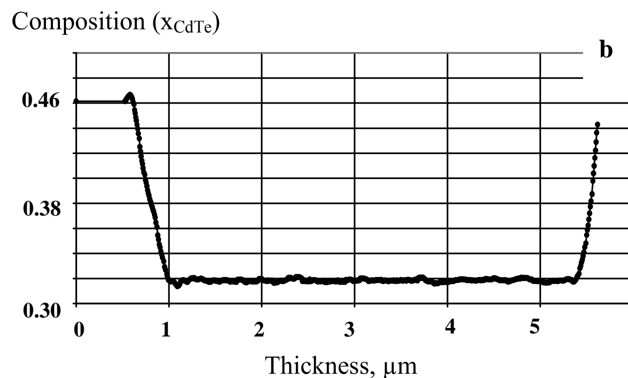

Fig. 1. (a) Cross-sectional view of the typical MBE grown HgCdTe-based heterostructure with photolithographically patterned contact metallization; (b) typical MCT composition profile throughout the thickness with wide bandgap layers at boundaries.

© 2012, V. Lashkaryov Institute of Semiconductor Physics, National Academy of Sciences of Ukraine

Table 1. Lattice parameters *a*, linear expansion coefficients α, and misfit between the parameters of the film and substrate for HgCdTe/CdTe and various substrates.

	a, nm at 300 K	α, 10^{-6} K^{-1}	Δ*a*/*a* (w/CdTe), %	α mismatch (w/CdTe), %
$Hg_{1-x}Cd_xTe$ (x = 0.24–0.3)	0.6464–0.6465	4.7	–	–
$Cd_{1-y}Zn_yTe$ (y = 0.04)	0.6464	5	0	0
CdTe	0.6481	5	0	0
ZnTe	0.610	8.29	6.2	60
GaAs	0.5642	5.8	14.6	13.8
Si	0.5431	2.6	19.3	92.3

Note. The lattice constant for $Hg_{1-x}Cd_xTe$ alloys used in the present analysis is given by [6]:
$a(x,T) = 6.4614 + 0.008x + 0.0168x^2 - 0.0057x^3 - 0.0095 + 2.613 \cdot T \cdot 10^{-5} + 1.131 \cdot T^2 \cdot 10^{-8}$.
For $Cd_{1-y}Zn_yTe$ with low zinc concentration, the lattice constant is assumed to be the same as for HgCdTe [7]: $a(y,T) = 6.4803 - 0.38y - 0.0095 + 2.613 \cdot T \cdot 10^{-5} + 1.131 \cdot T^2 \cdot 10^{-8}$.

Table 2. Some parameters of typically investigated HgCdTe epilayers, 78 K.

		Substrate	Layer thick-ness *d*, μm	*n*, cm^{-3}	μ_n, $\frac{cm^2}{V \cdot s}$	*p*, cm^{-3}	μ_p, $\frac{cm^2}{V \cdot s}$	Micro-hardness, GPa	Residual stresses, MPa
1	MBE x=0.3	(013)GaAs	8.9	$2 \cdot 10^{14}$	17000	–	–	0.28	
2	MBE x=0.235	(013)GaAs	14	$1.6 \cdot 10^{14}$	20000	–	–	0.288	~ –2
3	MBE x=0.32	(310)Si	5.6	$1.6 \cdot 10^{13}$	13000	10^{16}	230	1.12	~15
4	LPE x=0.26	(111) CdZnTe	12	–	–	$1.2 \cdot 10^{16}$	500	0.248	

Mechanical properties of MCT layers were evaluated from the microhardness measurements by the Vickers hardness test, which was performed with a Shimadzu HMV-2000. Data have been summarized in Table 2.

3. Results

3.1. Photosensitivity of MCT-based heterostructures at room temperature

Spectral response of the MBE- and LPE-grown structures was investigated at room temperature. Samples were illuminated from the film side in the wavelength region 1 to 16 μm. The IR source consisted of a globar heated at the temperature 1350 K. IR radiation was modulated by a mechanical chopper at the frequencies 40 to 338 Hz.

A voltage arising was recorded without electrical bias by using the lock-in nanovoltmeter in HgCdTe/Si heterostructure under IR photoexcitation. Contact metallization was photolithographically patterned on the structure top (Fig. 1a). The value of the photovoltage depends on the irradiation intensity *I* and its spectral composition *I* (λ). A spectral response of other structures grown on GaAs and CdZnTe substrates was insignificant.

Fig. 3a shows a single peak of the spectral sensitivity *S* at the wavelength 3 μm with the longwave sensitivity extended between 6 and 14 μm. The spectral sensitivity of the $Hg_{0.68}Cd_{0.32}Te$/Si heterostructure was measured in air (at 296 K). Here, the sample was mounted in clamps with low thermal conductivity. The dependence on the modulation frequency of the incident light was found. An increase in the modulation frequency from 40 up to 338 Hz results in the increase of the sensitivity value in MWIR region and the decrease it in LWIR region (see Fig. 3a). At the same time, there is no frequency dependence of the sensitivity for experiment carried out in evacuated chamber where sample was mounted on the bulk copper platform, see Fig. 3b. The reduction of temperature at the same modulation frequency increases the value of the spectral sensitivity in MWIR region.

Thus, $Hg_{1-x}Cd_xTe$/Si heterostructure with x~0.3 has shown photosensitivity in both MWIR and LWIR regions, which can be registered without electrical bias at room temperature.

3.2.Prototype of photovoltaic detector

Based on $Hg_{0.68}Cd_{0.32}Te$/Si heterostructure, we fabricated a device prototype with the light receiving area ~1 mm^2, the electrode area ~ 0.01 mm^2, and

© 2012, V. Lashkaryov Institute of Semiconductor Physics, National Academy of Sciences of Ukraine

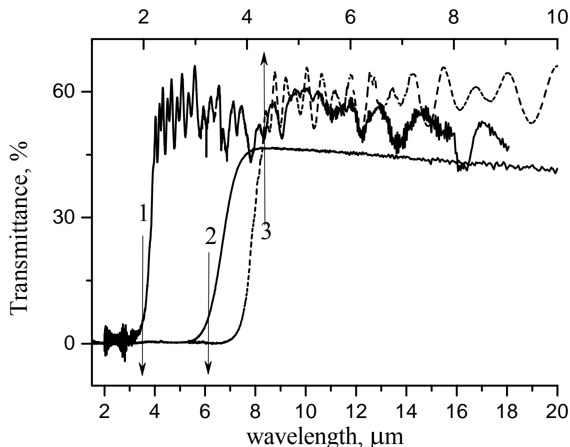

Fig. 2. Infrared transmittance spectra of the typical heterostructures: $Hg_{0.68}Cd_{0.32}Te/Si$ (*1*), $Hg_{0.74}Cd_{0.26}Te/Cd_{0.96}Zn_{0.04}Te$(*2*), $Hg_{0.7}Cd_{0.3}Te/GaAs$ (*3*).

interelectrode distance ~1 mm. Electrodes were patterned on the heterostructure top and protected from irradiation. Contact geometry was agreed by the piezoelectric field orientation in [310]-oriented structure. Resistance in a 1 mm^2 total area sensitive element was 1 kOhm.

To estimate the voltage responsivity, the prototype was exposed to infrared photons from a laser source (continuously operated He-Ne laser, LGN 113) with the wavelengths 0.63, 1.15, and 3.39 μm. The measured value of responsivity shown in Fig. 4 was from ~0.5 to ~4.3 V/W at 0.5 mW laser beam power in the focal spot. We also found out that the prototype of our photovoltaic detector is sensitive to CO_2 laser radiation on the level of ~0.04 V/W at 1 mW laser beam power in focal spot.

Since the prototype of our photovoltaic detector is not biased, the noise voltage is determined by the Johnson–Nyquist thermal noise. An element of the prototype achieves photovoltaic spectral sensitivity at the level $D^* = 2.6 \cdot 10^9\ W^{-1} cm \cdot Hz^{1/2}$ at 300 K and λ~3 μm.

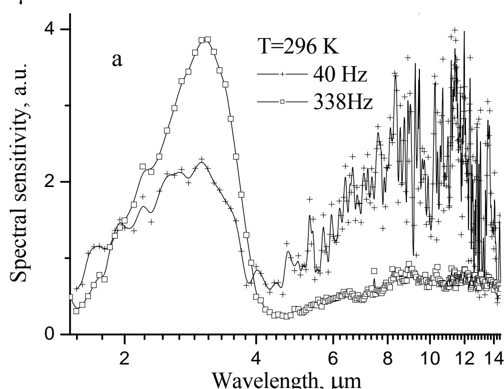

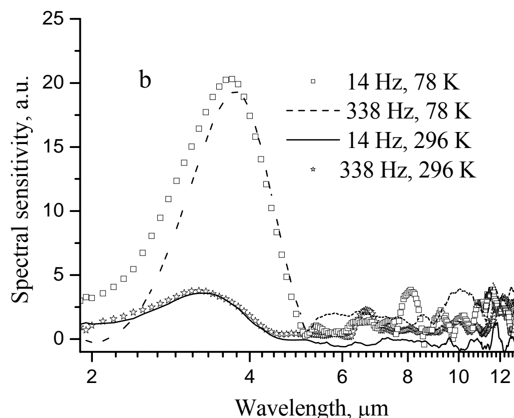

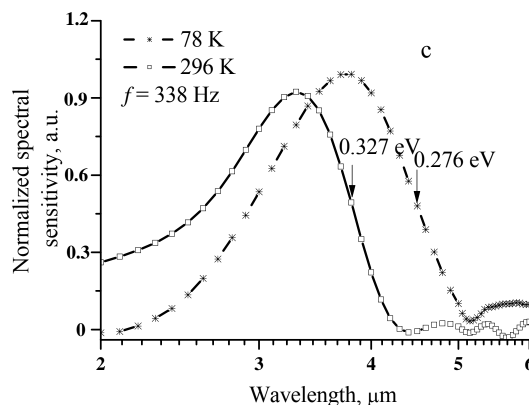

Fig. 3. Relative spectral sensitivity of the typical $Hg_{0.68}Cd_{0.32}Te/Si$ heterostructure. All the data have been normalized to the photoresponsivity of the standard piroelectric detector: a) spectra obtained in air; b) spectra obtained in the evacuated chamber; c) spectra obtained in the evacuated chamber and normalized to a maximum value.

4. Discussion

First of all, let us analyze some features of the spectral distribution of MCT-based device photosensitivity. A single peak of the spectral sensitivity *S* at the wavelength 3 μm is in good agreement with the region of the $Hg_{0.68}Cd_{0.32}Te$ fundamental absorption (see Fig. 3a and 3b) and is conditioned by electron processes apparently. The normalized spectrum shown in Fig. 3c is a selective peak with the spectral position of the “red” boundary, which corresponds to the band gap of MCT alloy with $x = 0.324$. Moreover, the longwave shift of the “red” boundary with temperature decrease corresponds to temperature narrowing the MCT bandgap.

The electron component of detector sensitivity reaches its maximum value for the time that corresponds well to the lifetime of photogenerated charge carriers in MCT crystal (~10^{-6} s at 300 K [2]), whereas the time scale of thermal effects is slower: their characteristic time constant is larger than 10^{-3} s. In our experiments, the time for which the detector surface was exposed to

© 2012, V. Lashkaryov Institute of Semiconductor Physics, National Academy of Sciences of Ukraine

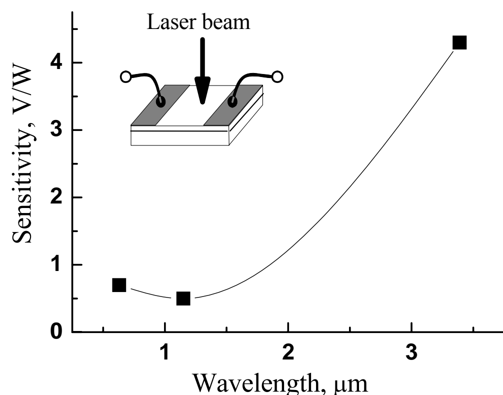

Fig. 4. Voltage responsivity of the prototype of photovoltaic detector based on HgCdTe/Si heterostructure.

photons was $(3-25)\times 10^{-3}$ s . In other words, the decrease in the sensitivity value in the 8…14-μm region (see Fig. 3a) at the increase of the modulation frequency from 40 up to 338 Hz is the evidence of thermal nature of the photoresponse for spectral region mentioned above.

Thus, our study allows thinking about the electron mechanism of the room temperature sensitivity of the MCT/Si-based detector in MWIR region and the thermal mechanism in LWIR spectral region. At the same time, it is well known that thermal processes dominate near room temperature in MCT-based devices used in the middle and longwave regions as well as in the conventional photon detector it is not possible to accurately detect any infrared radiation other than that of high output power as in a CO_2 gas laser. Conventional MCT-based photon detectors need significant cooling in order to reduce noise and leakage currents resulting from generation and recombination near room temperature.

Although the need for cooling has long been thought to be fundamental and inevitable, it has been recently suggested that Auger recombination and generation rates can be reduced by using the phenomena of exclusion and extraction to produce non-equilibrium carrier distributions [16]. Photodiode HgCdTe/Si structures based on this concept were manufactured for near-room temperature operation [5]. In addition, three types of IR photovoltaic detectors can operate at near-room temperature: photoelectromagnetic detectors, magnetoconcentration detectors, and Dember effect detectors [17]. The operation principle of these devices is based on the carrier separation as a result of a certain effect.

In our opinion, the possibility to detect infrared radiation by MCT-based structure investigated in this study without cryogenic cooling to achieve useful performance is based on the possibility of the spatial separation of non-equilibrium carriers in the stressed semiconductor heterostructure with the piezoelectric properties [14, 18].

It is worth noting that for compound heterostructures (such as HgCdTe/CdTe/ZnTe/Si or HgCdTe/CdTe/ZnTe/GaAs, observable here), the presence of residual stresses is a specific character caused by their physical nature. Mechanical stresses arise from various causes, including the physical nature of the as-deposited material, thermal expansion differences between the film and substrate materials, and chemical or structural changes occurring in the film in the course of processing.

It is obvious that the stresses in epilayers grown onto various substrates are different. We verified this statement by the investigation of the microhardness. The values of microhardness of MCT epilayers grown onto various substrates were found to lie within the range from 0.25 up to 1.12 GPa (see Table 2). The value of hardness of $Hg_{1-x}Cd_xTe$/Si is drastically higher than that for lattice matched $Hg_{1-x}Cd_xTe$/CdZnTe (sample 4, Table 2) or for annealed $Hg_{1-x}Cd_xTe$/GaAs (sample 1, Table 2).

Then, we estimated the residual stresses experimentally using the X-ray diffraction technique. Due to strain-induced bowing, Bragg peak positions will differ slightly in different points on the film surface. X-ray diffraction rocking curve full width at half-maximum mapping was used to generate a surface profile from which a radius of curvature (ΔR) is extracted. The change in radius, before and after layer structure deposition, can be used to estimate the residual film stresses from the Stoney formula:

$$\sigma_{\exp} = \frac{E_s d_s^2}{6(1-\nu_s)d_l}\frac{1}{\Delta R},$$

where d_l and d_s are the layer and substrate thicknesses, respectively, E_s and ν_s are the linear elastic modulus and Poisson's ratio of the substrate, respectively.

The absolute value of the experimentally determined stresses $\sigma_{\exp}$ for epitaxial systems under study reaches 2 to 15 MPa (see Table 2). These values are fairly similar to the data of ref. [20]. It should be noted that CdTe/ZnTe/GaAs structure is grown in compression, since the sign of $\sigma_{\exp}$ is negative, while for CdTe/ZnTe/Si structure, the total residual stresses are tensile. The ZnTe layer was ignored during stress analysis, since the presumption is that the thick CdTe layer should dominate the stress characteristics of the buffered substrate.

MCT alloys under normal conditions crystallize in $F43m$ lattice and show piezoelectric properties. For cubic symmetry, in principal coordinate axes, all the nonzero components of the piezoelectric tensor for $F43m$ lattice are equal: $e_{123} = e_{132} = e_{231} = e_{213} = e_{312} = e_{321} = e$ and for MCT $e = 0.0136$ C/m^2 [8]. Our previous study of the piezoelectric properties of MCT alloys [18] has shown that a piezoresponse does not arise $\left(P_i = e'_{ij}\varepsilon_j = 0\right)$, if the strains are of the form $\varepsilon_j = (\varepsilon\,\varepsilon\,\varepsilon\,0\,0\,0)^T$. For example, as in the case of homogeneous heating. If inhomogeneous boundary conditions are realized, where the substrate specifies the strain of MCT layer along the y_1 and y_2 axes and does not affect the strain along the y_3 axis, the strain tensor

© 2012, V. Lashkaryov Institute of Semiconductor Physics, National Academy of Sciences of Ukraine

will have the form $\varepsilon_j = (\varepsilon_{sub}\ \varepsilon_{sub}\ \varepsilon\ 0\ 0\ 0)^T$. Here, the induced polarization will differ from zero along the y_3 axis $\mathbf{P_3} = e'_{3j}\varepsilon_j = -0.45e(\varepsilon - \varepsilon_{sub})$. Thus, the piezoelectric charge is produced by mechanical stresses in semiconductor heterostructure.

It is worth noting that, for [100], [010], or [001]-oriented MCT layers, no piezoelectric polarization will be induced, while in the case of its orientation in the directions [111], [110] and [310], polarization has to appear in the layer [18].

It is well known that large built-in piezoelectric fields exceeding typically $10^5\ \mathrm{V\cdot cm^{-1}}$ are observed in strained piezoelectrically active heterostructures ($Ga_{1-x}In_xAs/GaAs$ [19], $CdTe/Cd_{1-x}Zn_xTe$ [20]) grown on a high-index surface. A piezoelectric field of $\sim 1840\ \mathrm{V\cdot cm^{-1}}$ is induced by the thermal stress from cryogenic cool (from 300 to 77 K) of HgCdTe/Si hybrid infrared devices fabricated on (111) HgCdTe surfaces [8].

In the case under consideration, residual stresses can induce the electric field within the range from 0.8 to $80\ \mathrm{V\cdot cm^{-1}}$ estimated according to $\mathbf{E_3} = -\mathbf{P_3}/\varepsilon\varepsilon_0$, where ε is the dielectric permittivity of MCT, and ε_0 is the vacuum electric constant. Apparently, it is need to take into account that wide gap layer at the MCT surface also creates built-in electric field, which is opposite to the direction of the piezoelectric field induced by compressive residual stresses in the heterostructure (MCT/…/GaAs). It can cancel the electrical field induced by residual stresses. On the other hand, the built-in electric field of the variband layer is directed in the same way as the piezoelectric field induced by tensile stresses (MCT/…/Si). The resultant field value will be reinforced.

It is also worth noting that such material as silicon has a centrosymmetric crystal structure and covalent bonding and in mechanical deformation does not affect the charge distribution. In other words, the influence of the silicon substrate on the resultant electrical field can be excluded in this heterostructure. Whereas gallium arsenide has acentric crystal symmetry, and the mechanical stress in this case results in an electrical imbalance.

It is obvious that the field caused by the piezoelectric effect of a conductive material is screened by free carriers inside the crystal. But, we think that piezoelectric field is available in the depletion region, where the carrier concentration is considerably lower than the intrinsic concentration for HgCdTe at 300 K.

Thus, existence of the built-in electric field in MCT-based heterostructure on the silicon substrate results in formation of the depletion region and spatial separation of electrons and holes. As a consequence, conditions for generation and the possibility of the room temperature photovoltage detection are implemented. At the same time, the built-in electric field in MCT/…/GaAs heterostructure is very likely compensated, and we cannot detect IR radiation at room temperature.

Our previous study has shown a significant role of the substrate properties for the stability of the MCT epilayers [21]. In this study, we can state about the substrate role for possibility of IR detection.

5. Conclusions

We have demonstrated HgCdTe-based IR detector operating in the middle (3 to 5 μm) and longwave (8 to 14 μm) infrared spectral range without cryogenic cooling to achieve useful performance. It was observed that $Hg_{0.68}Cd_{0.32}Te/CdTe/ZnTe/Si$ heterostructure obtained by MBE method exhibits photoresponse under IR photoexcitation without electrical bias. An element of the prototype achieves photovoltaic spectral sensitivity at the level $D^* = 2.6\cdot10^9\ \mathrm{W^{-1}cm\cdot Hz^{1/2}}$ at 300 K. The spectral response of the MCT-based structures grown on GaAs and CdZnTe substrates was insignificant.

The possibility to detect infrared radiation by using the MCT-based structure investigated in this study without cryogenic cooling to achieve useful performance is based on the possibility the spatial separation of the non-equilibrium carriers in the strained semiconductor heterostructure with piezoelectric properties. The substrate properties have been observed to play a significant role for observable principle of IR detection.

Acknowledgment

The authors are grateful to Dr V. Kladko for his helpful cooperation with the X-ray diffraction experiment.

References

1. A. Rogalski, *Infrared Detectors*, second ed. CRC Press, 2010.
2. M.V. Yakushev, V.S. Varavin, V.V. Vasiliev, S.A. Dvoretsky, I.V. Sabinina, U.G. Sidorov, A. Sorochkin, and A.L. Aseev, *Photodiodes*, ed. Jeong-Woo Park, InTech, 2011, p. 367-400.
3. S.M. Johnson, A.A. Buell, M.F. Vilela, J.M. Peterson, J.B. Varesi, M.D. Newton, G.M. Venzor, R.E. Bornfreund, W.A. Radford, E.P.G. Smith, J.P. Rosbeck, T.J. De Lyon, J.E. Jensen, and V. Nathan, HgCdTe/Si materials for long wavelength infrared detectors // *J. Electron. Mater.* **33**, p. 526-530 (2004).
4. T.D. Golding, O.W. Holland, M.J. Kim, J.H. Dinan, L.A. Almeida, J.M. Arias, J. Bajaj, H.D. Shih, and W.P. Kirk, HgCdTe on Si: Present status and novel buffer layer concepts // *J. Electron. Mater.* **32**, p. 882-889 (2003).

© 2012, V. Lashkaryov Institute of Semiconductor Physics, National Academy of Sciences of Ukraine

5. S. Velicu, G. Badano, Y. Selamet, C.H. Grein, J.P. Faurie, S. Sivananthan, P Boieriu, Don Rafol, and R. Ashokan, HgCdTe/CdTe/Si infrared photodetectors grown by MBE for near-room temperature operation // *J. Electron. Mater.* **30**, p. 711-720 (2001).
6. EMIS Data reviews Series *Properties of Narrow Gap Cadmium-Based Compounds,* N10, ed. P. Capper. London: INSPEC, 1994, p. 41.
7. M.A. Berding, W.D. Nix, D.R. Rhiger, S. Sen, and A. Sher, Critical thickness in the HgCdTe/CdZnTe system // *J. Electron. Mater.* **29**, p. 676-679 (2000).
8. C.F. Wan, J.D. Luttmer, R.S. List, and R.L. Strong, Piezoelectric effects in HgCdTe devices // *J. Electron. Mater.* **24**, p. 1293-1297 (1995).
9. A. T. Paxton, A. Sher, M. Berding, M. Van Schilfgaarde and M.W. Muller, How dislocations affect transport // *J. Electron. Mater.* **24**. p. 525-532 (1995).
10. V. Ortiz, N.T. Pelekanos, and G. Mula, Efficient all-optical light modulation in a piezoelectric heterostructure at room temperature // *Appl. Phys. Lett.* **72**, p. 963-965 (1998).
11. D.L. Smith, Piezoelectric effects in strained layer heterostructures grown on novel index substrates // *Microelectron. J.* **28**, p. 707-715 (1997).
12. Peng Fei, Ping-Hung Yeh, Jun Zhou, Sheng Xu, Yifan Gao, Jinhui Song, Yudong Gu, Yanyi Huang, and Zhong Lin Wang, Piezoelectric potential gated field-effect transistor based on a free-standing ZnO wire// *Nano Lett.* **9**, p. 3435-3439 (2009).
13. S. Patil, B. Wen and R.V.N. Melnik, Strain effects and temperature-dependent phase stability of II-VI semiconductor nanostructures // *AIP Conf. Proc.* **1199**, p. 303-304 (2010).
14. *Ukrainian patent* UA40000, F.F. Sizov, R.K. Savkina, and A.B. Smirnov, Uncooled photovoltaic detector of IR radiation. Promyslova vlasnist', No.6, 2009.
15. A.V. Voitsekhovskii, D.V. Grigor'ev, A.G. Korotaev and A.P. Kokhanenko, Specific features of determining the electrophysical parameters of variband CMT structures grown by molecular-beam epitaxy // *Russian Physics Journal*, **47**, p. 764-772 (2004).
16. T. Ashley, C.T. Elliott, and A.T. Harker, Non-equilibrium modes of operation for infrared detectors // *Infrared Phys.* **26**, p. 303-315 (1986).
17. J. Piotrowski and A. Rogalski, Uncooled long wavelength infrared photon detectors // *Infrared Phys. Technol.* **46**, p. 115-131 (2004).
18. R.K. Savkina, F.F. Sizov, A.B. Smirnov, M.V. Yakushev and V.A. Deriglazov, IR uncooled photovoltaic cell on basis of $Cd_xHg_{1-x}Te/Si$ ($x = 0.3$) // *Prikladnaya Fizika* **4**, p. 58-64 (2011), in Russian (www.vimi.ru/applphys/).
19. E.A. Caridi, T.Y. Chang, K.W. Goossen, and L. Eastman, Direct demonstration of a misfit strain-generated electric field in a [111] growth axis zinc-blende heterostructure // *Appl. Phys. Lett.* **56**, p. 659-661 (1990).
20. R. Andre, C. Deshayes, J. Cibert, L.S. Dang, S. Tatarenko and K. Saminadayar, Optical studies of the piezoelectric effect in (111)-oriented $CdTe/Cd_{1-x}Zn_xTe$ strained quantum wells // *Phys. Rev. B*, **42**, p. 11392-11395 (1990).
21. R.K. Savkina, A.B. Smirnov and F.F. Sizov, The effect of high-frequency sonication on charge carrier transport in LPE and MBE HgCdTe layers // *Semicond. Sci. Technol.* **22**, p. 97-102 (2007).

© 2012, V. Lashkaryov Institute of Semiconductor Physics, National Academy of Sciences of Ukraine